Hindawi
Stem Cells International
Volume 2019, Article ID 7028901, 20 pages
https://doi.org/10.1155/2019/7028901

Research Article

The DNMT1/miR-34a Axis Is Involved in the Stemness of Human Osteosarcoma Cells and Derived Stem-Like Cells

Xiao Liang,[1] Chang Xu,[2] Wanchun Wang,[1] and Xiang Li[2]

[1]*Department of Orthopaedics, The Second Xiangya Hospital, Central South University, 139 Renmin Road, Changsha, Hunan 410011, China*
[2]*Department of Preclinical Medicine, Medical College, Hunan Normal University, Changsha, Hunan 410013, China*

Correspondence should be addressed to Wanchun Wang; wanchun.wang@csu.edu.cn and Xiang Li; lx58616@163.com

Received 10 May 2019; Accepted 25 September 2019; Published 31 October 2019

Academic Editor: Valeria Sorrenti

The DNA methyltransferase 1 (DNMT1)/miR-34a axis promoted carcinogenesis of various types of cancers. However, no literature reported its contribution to the stemness of osteosarcoma cancer stem-like cells (OSLCs). We sought to determine whether the DNMT1/miR-34a axis facilitates the stemness of OSLCs. We here revealed the higher DNMT1 activity and expression, lower miR-34a expression with high methylation of its promoter, and stronger stemness of OSLCs, as manifested by elevated sphere and colony formation capacities; CD133, CD44, ABCG2, Bmi1, Sox2, and Oct4 protein amounts *in vitro*; and carcinogenicity in a nude mouse xenograft model, when compared to the parental U2OS cells. 5-Azacytidine (Aza-dC) repressed DNMT1 activation and upregulated miR-34a expression by promoter demethylation and suppressed the stemness of OSLCs in a dose-dependent manner. DNMT1 knockdown increased miR-34a and reduced the stemness of OSLCs. Transfection with a miR-34a mimic repressed the stemness of OSLCs but did not alter DNMT1 activity and expression. Conversely, DNMT1 overexpression declined miR-34a levels, promoting the stemness of U2OS cells. Transfection with a miR-34a inhibitor enhanced the stemness of U2OS cells, without affecting the DNMT1 activity and expression. Importantly, reexpression of miR-34a could rescue the effects of DNMT1 overexpression on miR-34a inhibition as well as the stemness promotion without affecting the activity and expression of DNMT1. Our results revealed that aberrant activation of DNMT1 caused promoter methylation of miR-34a, leading to miR-34a underexpression, and the role of the DNMT1/miR-34a axis in promoting and sustaining the stemness of OSLCs.

1. Introduction

Osteosarcoma (OS) is the most common bone-derived solid cancer in children and adolescents and originates from mesenchymal cells of osteoblast origin [1, 2]. The long-term survival of OS patients remains to have no significant improvements due to metastases and chemoresistance [3]. Accumulating evidence supported the notion that a small subpopulation of cells with stem-like characteristics called cancer stem-like cells (CSLCs) are the most cause for cancer metastasis and chemoresistance owing to their stronger stemness [4]. Therefore, it is necessary to urgently clarify the underlying cellular and molecular mechanisms to facilitate and sustain the stemness of OS cells.

MicroRNAs (miRNAs) regulate the function and property of CSLCs, and dysregulation was involved in the stemness of prostate cancer and Ewing's sarcoma [5, 6]. For instance, downregulated miR-200b, miR-200c, and miR-145 act as tumor suppressors in the upregulation of pluripotency in maintaining factors, such as Bmi1, Oct4, c-Myc, and Sox2, thereby conferring the capacities of self-renewability and colony formation in CSLCs [7]. Recent studies have reported that miR-34a is underexpressed in various cancers such as Ewing's sarcoma [8], colorectal cancer [9], and OS [10, 11]. miR-34a also regulated colon CSLCs [12] and inhibited breast cancer stemness [13]. Liu et al. demonstrated that miR-34a inhibits prostate CSLCs by directly repressing CD44 [14]. The study by Zhang et al. [15] revealed that

human urothelial bladder cancer stemness was reduced by miR-34a. According to a recent study by Zou et al., the elevated self-renewal ability of human OS stem-like cells (OSLCs) was involved in miR-34a underexpression of these cells [11]. Despite the above studies on miR-34a, the upstream event and regulation of miR-34a in OSLCs are still unclear.

Most recent studies showed that epigenetic modifications are responsible for cancer initiation and progression by regulating the stemness of CSLCs [16–18]. Aberrant DNA methylation promotes the self-renewable capacity of ovarian CSLCs [16, 19]. DNA methyltransferase 1 (DNMT1) contributed to the maintenance of stemness of various CSLCs [20–25], including OSLCs [10, 11]. According to a study using mammary gland-specific DNMT1-knockout mice, DNMT1 deletion limited the CSLC population and reduced mammary tumorigenesis [20]. Notably, tumor-suppressive miRNAs could be silenced by DNA hypermethylation in the promoter regions [26–29]. Recent studies showed that miR-34a promoter hypermethylation led to epigenetic inactivation [30–33]. Considering the regulation of stemness of OSLCs by miR-34a [10, 11], we hypothesized that it may be possible to repress the stemness by upregulating miR-34a through inactivating DNMT1 in human OS cells and their derived OSLCs. We here sought to determine whether the DNMT1/miR-34a axis promotes the stemness of OSLCs.

2. Materials and Methods

2.1. Cell and Sphere Culture. Human osteosarcoma U2OS cells (Cell Bank of Chinese Academy of Sciences, Shanghai, China) were maintained in Dulbecco's modified Eagle's medium (DMEM; Gibco, Grand Island, NY, USA) containing 10% fetal bovine serum (FBS, Gibco) and penicillin (100 IU/ml)/streptomycin (100 μg/ml) at 37°C in 5% CO_2.

For sphere culture, U2OS cells (1×10^3) were suspended in the cancer stem cell-conditioned medium (CSC-CM) composed of serum-free DMEM/F12 (Invitrogen, Carlsbad, CA, USA) with 100 IU/ml penicillin, 100 μg/ml streptomycin, 20 ng/ml hrEGF (Invitrogen), 20 ng/ml hbFGF (Invitrogen), 2% B27 (Invitrogen), 0.4% BSA (Invitrogen), and 4 μg/ml insulin (Sigma-Aldrich) to form spheres. The sphere-forming U2OS cells obtained from the sphere formation culture were called OSLCs as described by Zou et al. [11].

2.2. DNMT1 Activity Detection. Nuclear extracts from OSLCs (1×10^6) or U2OS cells (1×10^6) were obtained by the EpiQuik™ Nuclear Extraction Kit (cat. OP-0002-1; EpiGentek Group Inc., Farmingdale, NY, USA). DNMT1 activity is nonradioactively measured by using a DNA Methyltransferase Activity/Inhibition Assay Kit (cat. P-3001; EpiGentek Group Inc., Farmingdale, NY, USA) according to the protocol. DNMT activity was calculated by using the formula, which was as follows: DNMT activity (OD/h/mg) = (no inhibitor OD − blank OD) 1000/protein amount (μg) × hour. Relative activity of DNMT1 was normalized by the activity of U2OS cells or untreated OSLCs.

2.3. Western Blot Analysis. The lysates were prepared by RIPA lysis buffer (Beyotime Institute of Biotechnology, Shanghai, China) from U2OS cells (1×10^6) or OSLCs (1×10^6). The protein concentrations were determined by the Bradford assay (Bio-Rad Laboratories, Hercules, CA, USA). Electrophoresis with sodium dodecyl sulfate-polyacrylamide gel (10%, SDS-PAGE) was used to separate the lysate (40 μg protein), which was then transferred onto a polyvinylidene fluoride (PVDF) membrane (Millipore). The membranes were then blocked with TBST containing 5% BSA for 2 h at room temperature and then incubated with primary antibodies anti-β-actin (1 : 5000; catalog no. A5441; Sigma-Aldrich), anti-CD133, anti-CD44, anti-ABCG2, anti-DNMT1, anti-Bmi1, anti-Sox2, and anti-OCT4 (1 : 2000; catalog nos. 5860S, 3570S, 4477S, 3598S, 5856, 2748, and 2840 CST) overnight at 4°C. The membranes were then incubated with appropriate HRP-conjugated secondary antibodies (Beyotime Institute) for 1 h. The protein bands were visualized using an enhanced chemiluminescence kit (Amersham Biosciences) by using an enhanced chemiluminescence detection system (Ranon GIS-2008, Tanon Science & Technology Co., Ltd., Shanghai, China).

2.4. Quantitative Real-Time PCR. Total RNA from U2OS cells (1×10^6) or OSLCs (1×10^6) was extracted using the TRIzol universal reagent (cat. DP424, Tiangen Biotech, Beijing, China), and miRNA was obtained by a miRcute miRNA isolation kit (cat. DP501, Tiangen Biotech, Beijing, China) following the manufacturer's instructions.

For mRNA detection, total RNA (2 μg) was transcribed into cDNA using the SureScript™ first-strand cDNA synthesis kit (cat. QP057, GeneCopoeia Inc., Maryland, USA). The BlazeTaq™ One-Step SYBR Green qRT-PCR kit (cat. QP047, GeneCopoeia Inc., Maryland, USA) was employed to amplify cDNA on a CFX Connect fluorescent quantitative PCR analyzer (Bio-Rad Laboratories). The primers used are listed in Supplementary Table S1. The cycling variables were set as follows: 95°C for 10 min, followed by 35 cycles of 95°C (30 sec), 55°C (30 sec), and 70°C (30 sec). Human β-actin RNA was used as an internal control for RNA normalization.

For determination of microRNA, miRNA (2 μg) was transcribed into cDNA using the All-in-One™ miRNA qRT-PCR detection kit (cat. QP016, GeneCopoeia Inc., Maryland, USA) including the All-in-One miRNA qRT-PCR detection kits and the All-in-One miRNA first-strand cDNA synthesis kits. U6 RNA was used as an internal control. Primers used are depicted in Supplementary Table S2. The results were analyzed by the method of $2^{-\Delta\Delta Ct}$.

2.5. Methylation-Specific PCR (MSP). Cellular DNA of U2OS cells (1×10^6) or OSLCs (1×10^6) was isolated using DNA-EZ reagents V All-DNA-Out (Sangon Biotech, Shanghai, China). Genomic DNA was treated with the Methylamp One-Step DNA Modification Kit (EpiGentek, NY, USA) following the manufacturer's instructions. HotStarTaq Polymerase (Qiagen, Germany) was used to amplify PCR, and Sangon Biotech Co., Ltd. (Shanghai, China) designed and provided the methylated and unmethylated PCR primers to determine the methylation of the miR-34a promoter. The

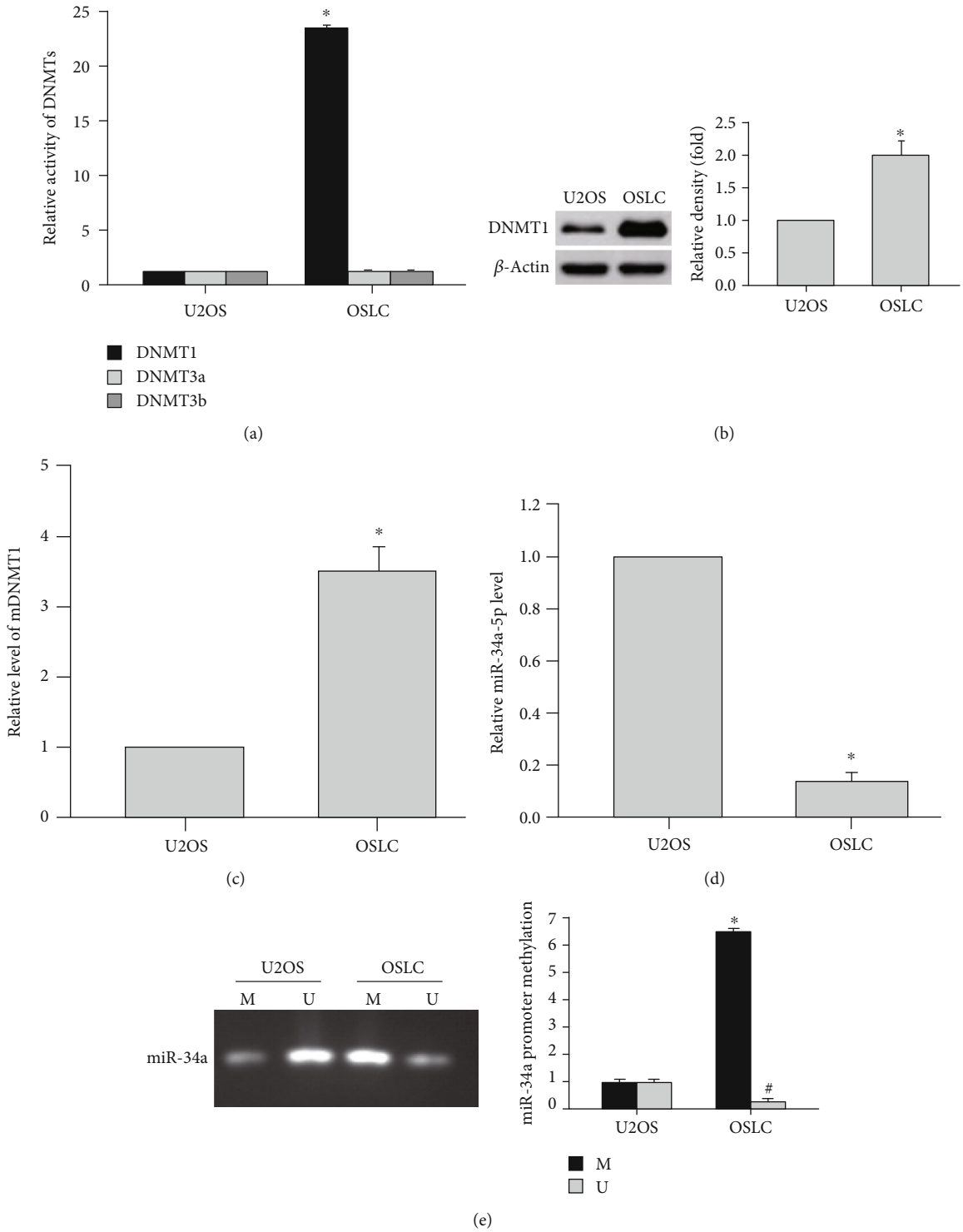

Figure 1: Continued.

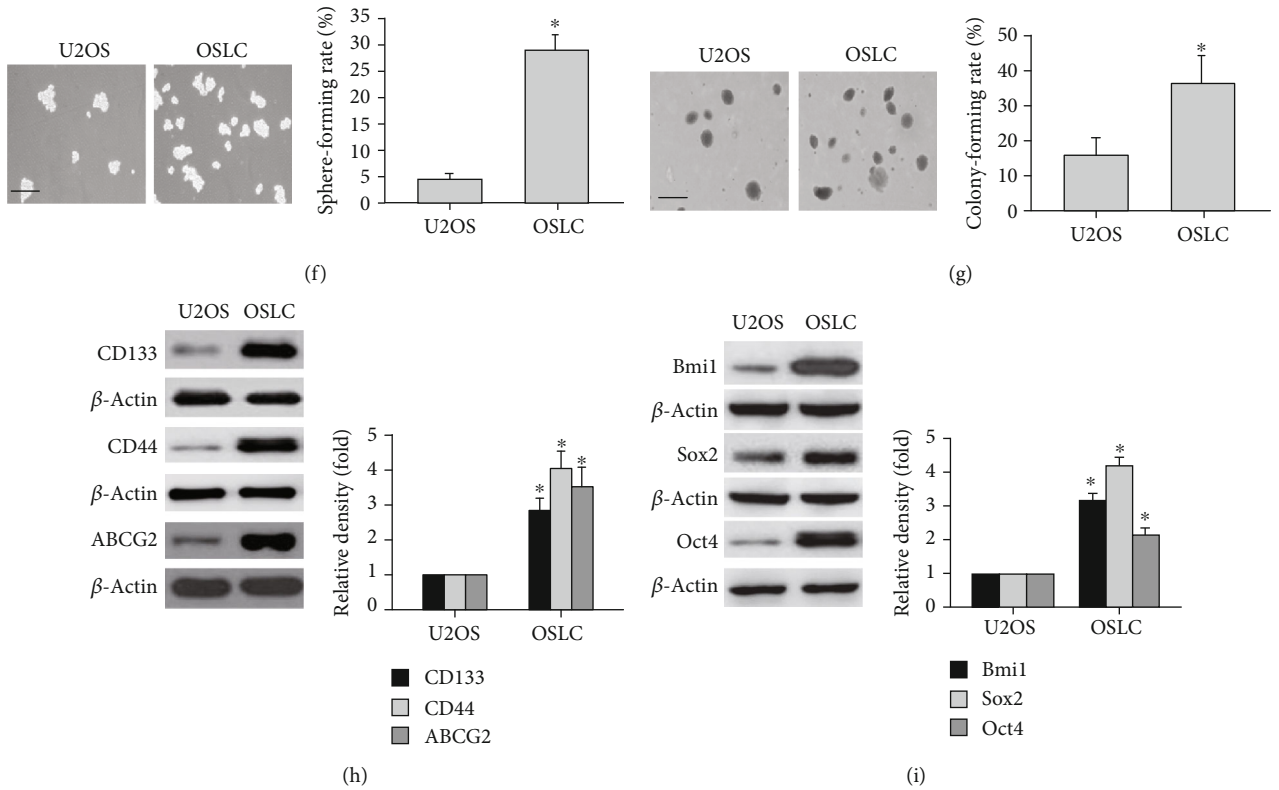

Figure 1: Comparison of stemness between U2OS cells and OSLCs. (a) The activity of DNMTs was determined by ELISA. (b) The level of DNMT1 protein was examined by immunoblot (left) and its densitometric analysis (right), with β-actin as a loading control. (c, d) DNMT1 mRNA and miR-34a-5p were assessed by qRT-PCR. (e) Comparison of miR-34a-5p promoter methylation levels in U2OS cells and OSLCs (M, methylated miR-34a-5p promoter; U, unmethylated miR-34a-5p promoter). (f) Representative images of sphere formation (left) (scale bar, 200 μm), and sphere-forming rate was assessed by the sphere formation assay (right). (g) Representative images of colony formation (left) (scale bar, 200 μm), and colony-forming rate was determined by the colony formation assay (right). (h) The levels of CD133, CD44, and ABCG2 proteins were examined by immunoblot (left) and their densitometric analysis (right). (i) Bmi1, Sox2, and Oct4 mRNA were assessed, with β-actin serving as a loading control. $^*p < 0.05$ ($n = 3$) vs. U2OS cells.

sequences of PCR primers specific for methylated and unmethylated alleles of miR-34a are shown in Supplementary Table S3. The products of MSP were visualized by 2.0% agarose gel electrophoresis (0.5 μg/ml ethidium bromide). UV gel electrophoresis and an image analysis system (Tanon 1600 full-automatic digital gel image analysis system) were used for image analysis.

2.6. Sphere-Forming Rate Assay. U2OS cells (1×10^3) or OSLCs (1×10^3) were suspended in CSC-CM and then cultured for 12 days until the spheres exceeded 20 cells. The total number of tumor spheres was counted. The sphere formation rate (%) was calculated as follows: (number of spheres formed/number of cells seeded) $\times$ 100.

2.7. Clonogenic Assay. The mixture containing 1.6% agarose (Invitrogen, Carlsbad, CA, USA) and DMEM (1 : 1, *v*/*v*) was added into a 6-well plate (per well 1 ml) as the bottom layer. Then, the top layer was composed of the mixture with CSC-CM containing MHCC97H cells (1×10^4) or LCSLCs (1×10^4) and 0.8% agarose (1 : 1) and placed over the bottom layer. Colonies were counted by using an inverted microscope (IX53; Olympus, Tokyo, Japan) after 3 weeks.

2.8. Lentivirus Infection and miRNA Transfection. Lentiviruses of LV-15 (pGLVH1/RFP/Puro) vectors carrying shRNA targeting human DNMT1 and lentiviruses of LV8N (EF-1αF/mCherry/Puro) vectors carrying human DNMT1 cDNA were purchased from GenePharma (Shanghai). OSLCs (1×10^5) or U2OS cells (1×10^5) in an exponential growth period were infected for 48 h with lentiviruses expressing DNMT1 shRNA or DNMT1 cDNA or RFP constructs in a medium containing 8 μg/ml polybrene for 48 h. The cells were selected with 4 μg/ml puromycin and maintained with 1 μg/ml puromycin. qRT-PCR was used to analyze DNMT1 mRNA expression in OSLCs expressing DNMT1 shRNA or U2OS cells expressing DNMT1 cDNA or RFP constructs. DNMT1 protein expression was assessed by immunoblot with an anti-DNMT1 antibody.

micr*ON*™ *miR-34a* mimic/micr*OFF*™ *miR-34a* inhibitors were obtained from RiboBio (Guangzhou, China) and were transfected into OSLCs or U2OS cells with the ibo*FECT*™ CP reagent (RiboBio Co., Ltd., Guangzhou, China) at a final concentration of 50/100 nM following the manufacturer's instructions. The transfection protocol for *miR-34a* mimic NC/*miR-34a* inhibitor NC that served as a

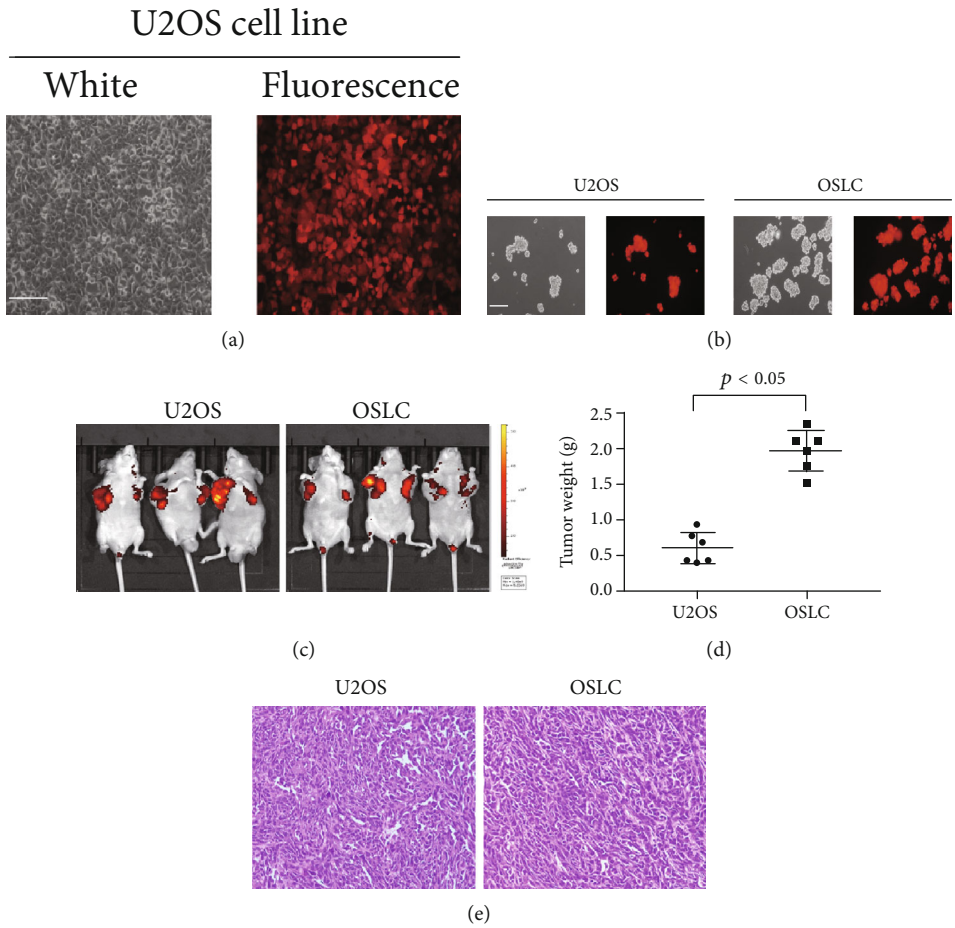

FIGURE 2: Comparison of carcinogenicity *in vivo* between U2OS cells and OSLCs. (a) Fluorescence microscopy image of U2OS cells that stably express red fluorescent protein (RFP, scale bar, 100 μm). (b) Fluorescence microscopy image of the spheres derived from U2OS cells and OSLCs that stably express RFP (scale bar, 100 μm). (c) Images of subcutaneous xenografts inoculating U2OS cells (2×10^5, injected into the left flank) or the corresponding OSLCs (2×10^3, injected into the right flank), which express RFP. (d) Comparison of the growth of xenografts from U2OS cells expressing red RFP (2×10^5) and the corresponding OSLCs (2×10^3). $^*p < 0.05$ vs. U2OS cells. Data were obtained from xenografts weighing results at 6 inoculated sites ($n = 6$). (e) Comparison of histological morphology of xenografts between U2OS cells (2×10^5) and U2OS-derived OSLCs (2×10^3). Images of HE staining under an optical microscope (scale bar, 100 μm).

negative control was the same as that for *miR-34a-5p* mimic/inhibitors.

2.9. In Vivo Tumorigenicity Experiments. Hunan Silaike Jingda Laboratory Animal Co., Ltd. (Changsha, China) provided the male BALB/c-nude mice (age, 4-5 weeks; body weight, 12-14 g) which were used in this study. The Ethics Committee of Hunan Normal University and the Committee of Experimental Animal Feeding and Management approved the experimental procedure.

For the *in vivo* tumorigenicity assay, mice ($n = 6$) were subcutaneously injected with U2OS cells that stably express red fluorescein protein (1×10^5) into the left flank and the corresponding OSLCs (1×10^3) into the right flank, respectively. After 2 months, the mice were euthanized and xenografts were collected. The xenografts were weighed after extraction, and the largest diameters exceeded 1.5 cm of OSLC xenografts.

To estimate the effect of DNMT1 inhibition on the tumor growth derived from OSLCs *in vivo*, the mice were subcutaneously injected with 100 μl phosphate buffer (PBS) containing OSLCs stably expressing DNMT1 shRNA or red fluorescein protein (1×10^5 cells). Each group was composed of 3 mice with 6 sites ($n = 6$).

To examine the effect of miR-34a on tumor growth of OSLCs *in vivo*, the mice were subcutaneously injected with 100 μl PBS containing OSLCs stably expressing red fluorescein protein (1×10^5 cells). When the xenograft size exceeded 200 mm^3, the mice were weekly intratumorally injected with 1 nmol (in 50 μl PBS) per site of micrON™ *agomir-34a* (RiboBio Co., Ltd., Guangzhou, China) in a total of 3 times as the experiment group and micrON™ *agomir-NC* as the control group constituting 3 mice at 6 sites ($n = 6$) in each group. We monitored the tumor size using the IVIS Lumina III *in vivo* imaging system (PerkinElmer Inc., NY, USA), and then, it was photographed. The shooting mode was kept as

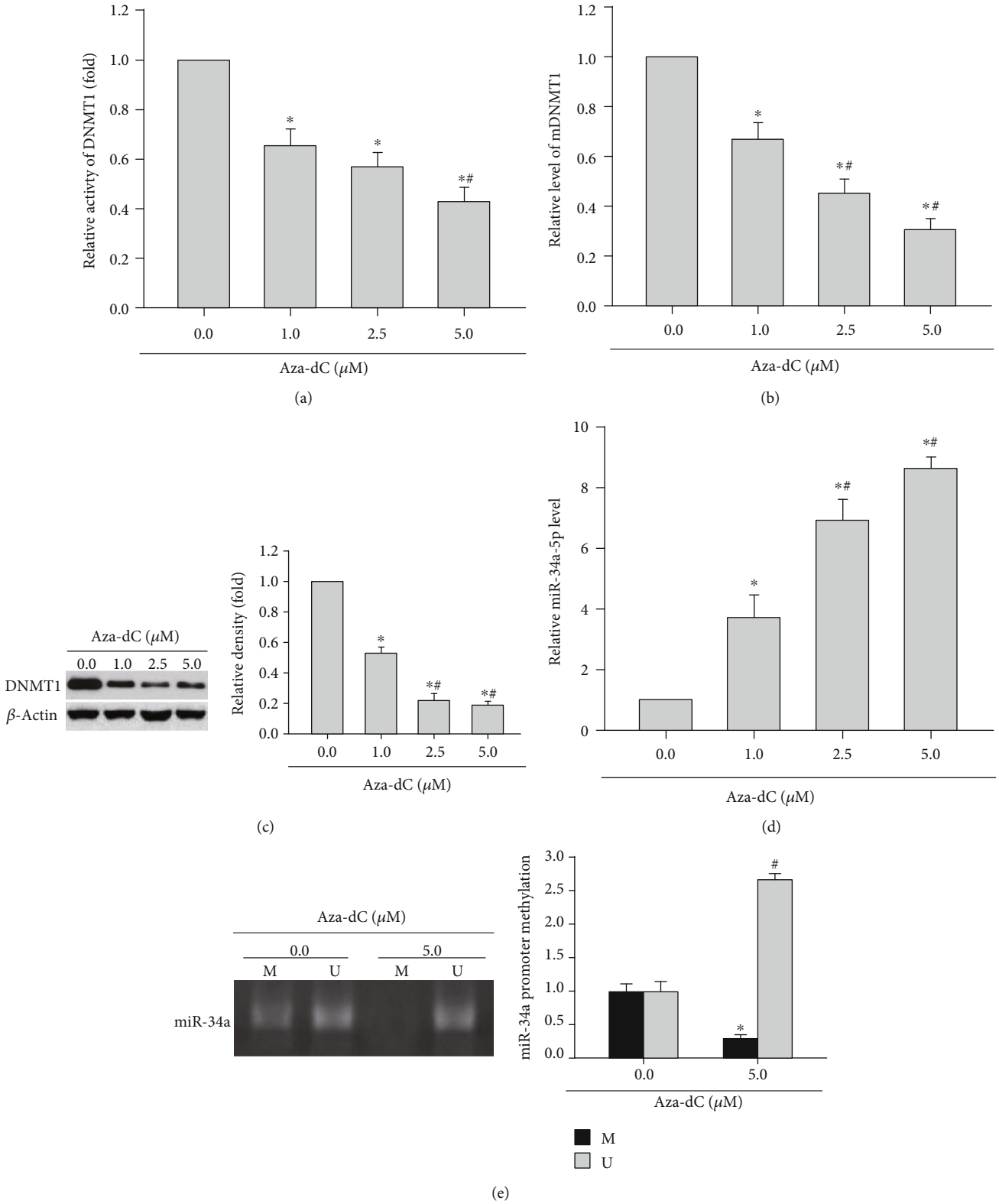

Figure 3: Continued.

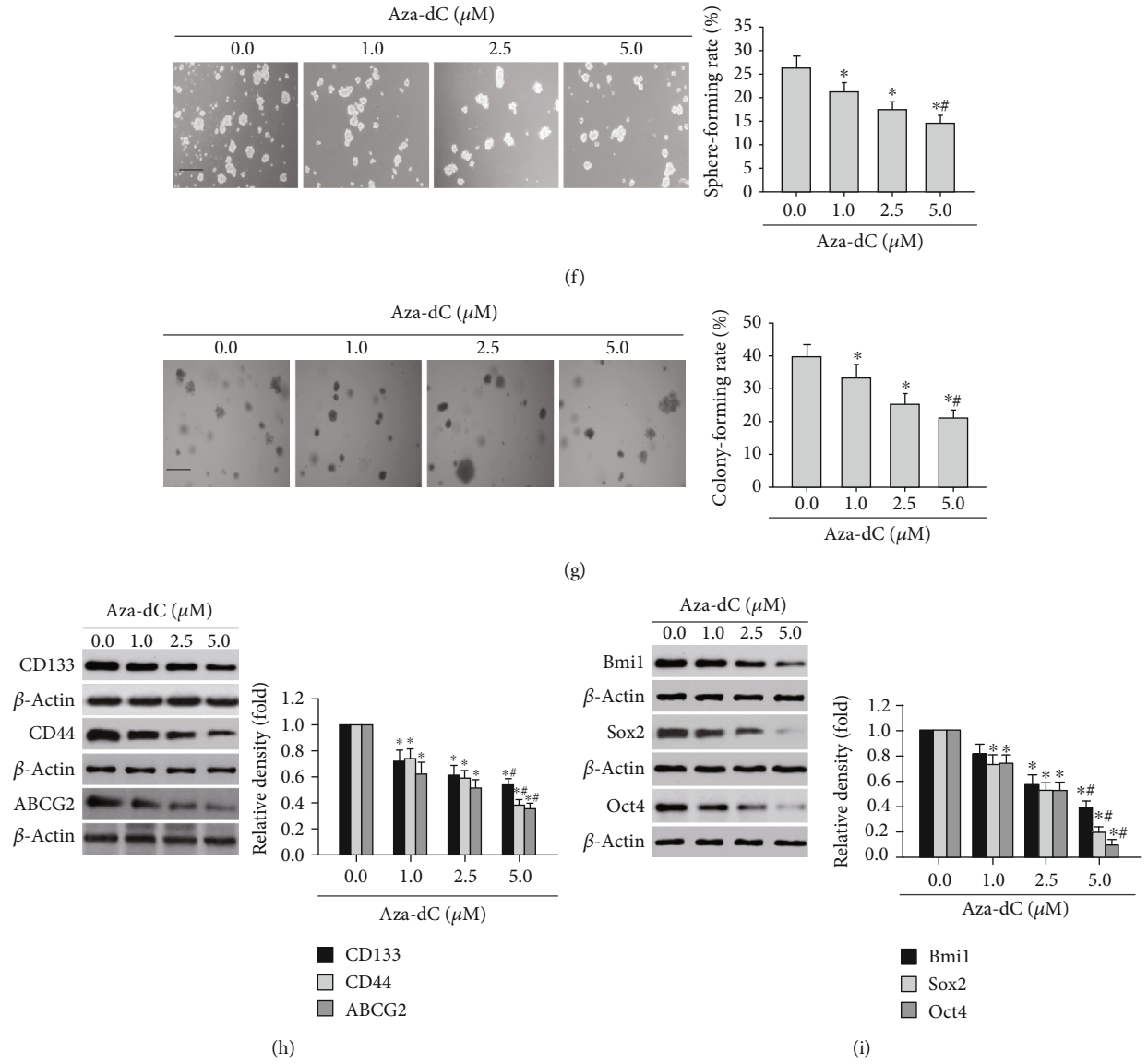

Figure 3: Effects of Aza-dC on the stemness feature in OSLCs. (a) The activity of DNMT1 in OSLCs treated with Aza-dC was assessed by ELISA. (b) The level of DNMT1 mRNA of OSLCs treated with Aza-dC was determined by qRT-PCR. (c) Immunoblotting was used to analyze the expression of DNMT1 of OSLCs treated with Aza-dC (left), as well as its densitometric analysis (right), with β-actin serving as a loading control. (d) The miR-34a-5p level of OSLCs treated with Aza-dC was detected by qRT-PCR. (e) The effect of Aza-dC on OSLC miR-34a-5p promoter methylation (M, methylated miR-34a-5p promoter; U, unmethylated miR-34a-5p promoter). (f) Representative images of the sphere formation of OSLCs treated with Aza-dC (left) (scale bar, 200 μm), and the sphere formation assay was used to assess the sphere-forming rate (right). (g) Representative images of the colony formation of OSLCs treated with Aza-dC (left) (scale bar, 200 μm), and the colony-forming rate of OSLCs was determined by the colony formation assay (right). (h) CD133, CD44, and ABCG2 proteins of OSLCs treated with Aza-dC (left) and their densitometric analysis (right). (i) Bmi1, Sox2, and Oct4 of OSLCs treated with Aza-dC. $^{*}p < 0.05$ ($n = 3$) vs. the DMSO control; $^{\#}p < 0.05$ ($n = 3$) vs. OSLCs treated with Aza-dC (1.0 μM).

fluorescence mode, with a peak wavelength of excitation of 587 nm and with a peak wavelength of emission of 610 nm, and the exposure time was 0.1 s. The fluorescence intensity was recorded and analyzed by living images by *in vivo* imaging software (PerkinElmer Inc., NY, USA). The xenografts were extracted, weighed, and frozen or fixed for further analysis.

2.10. Immunohistochemical Staining. Immunohistochemical staining was performed according to the standard procedures. Tissue slides were incubated at 4°C overnight with an anti-*DNMT1* antibody (1 : 200; DNMT1, catalog no. 3598S, Cell Signaling Technology). For negative controls, phosphate-buffered saline (PBS) was used instead of the primary antibody to detect the nonspecific reactions or false positives. Images were acquired by using the Olympus BX60 microscope (Olympus, Japan).

2.11. Statistical Analysis. Data were analyzed by SPSS 20.0 software (IBM, Armonk, NY, USA) and depicted as

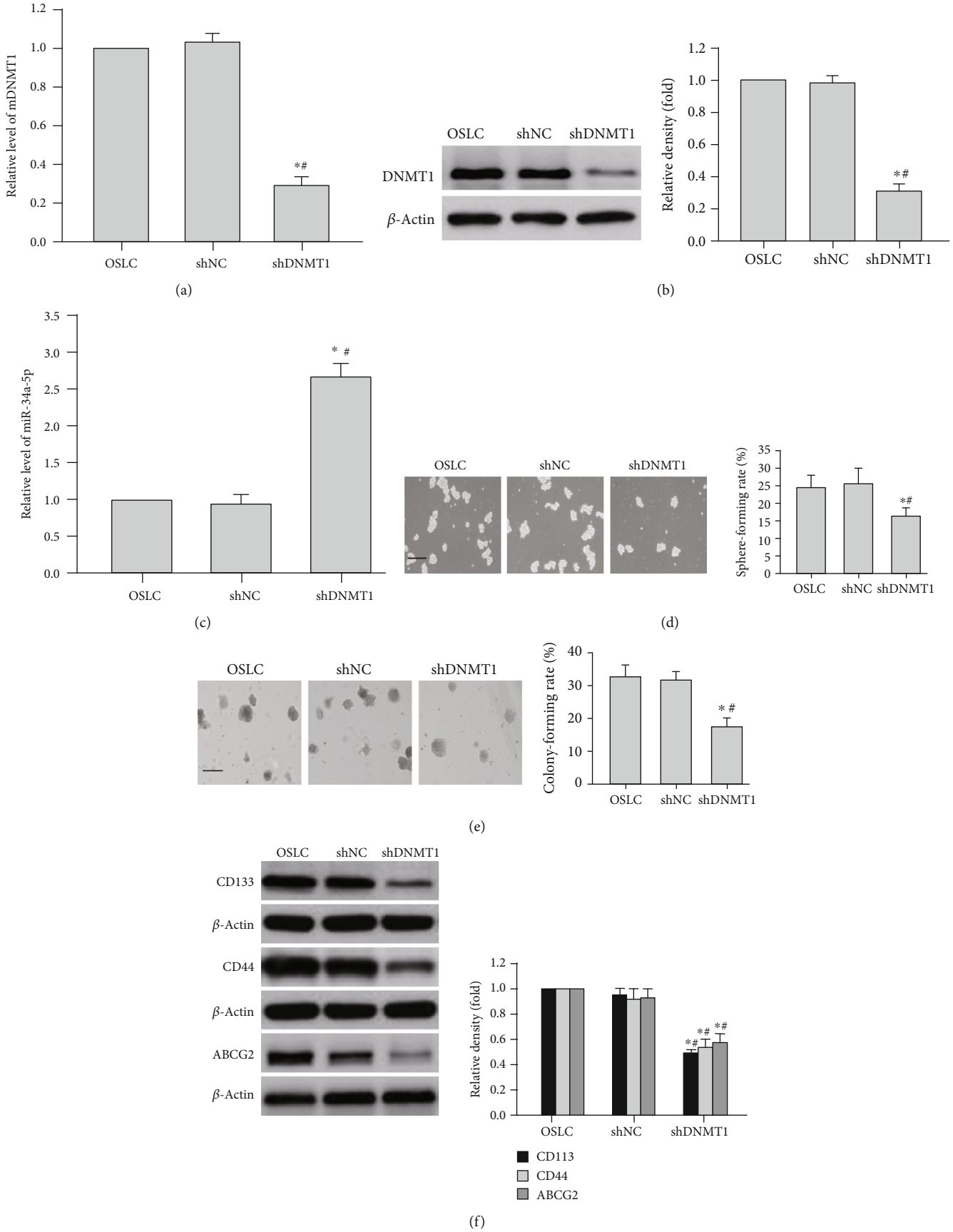

Figure 4: Continued.

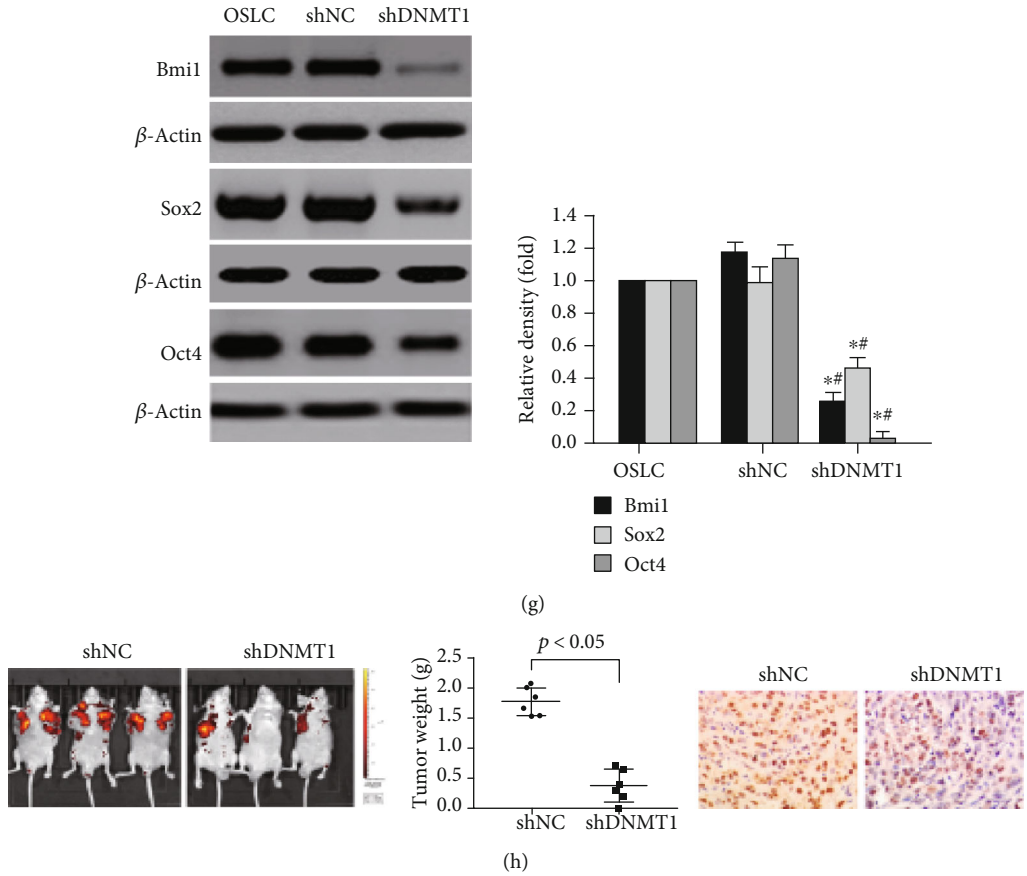

Figure 4: Effects of DNMT1 knockdown on the stemness feature in OSLCs. (a, b) qRT-PCR and immunoblot were performed to detect DNMT1 mRNA and protein in OSLCs transfected with shRNA DNMT1, respectively, with β-actin serving as a loading control. (c) qRT-PCR analyzed miR-34a-5p expression in OSLCs knocking down DNMT1. (d) Representative images of the spheres of OSLCs transfected with shNC or shDNMT1 (left) (scale bar, 200 μm) and sphere-forming rate (right). (e) Representative images of the colonies of OSLCs transfected with NC or DNMT1 shRNA (left) (scale bar, 200 μm) and colony-forming rate (right). (f) CD133, CD44, and ABCG2 proteins in OSLCs transfected with shNC or shDNMT1 (left) and their densitometric analysis (right). (g) Bmi1, Sox2, and Oct4 in OSLCs transfected with shNC or shDNMT1. $^{*}p < 0.05$ ($n = 3$) vs. U2OS cell; $^{\#}p < 0.05$ ($n = 3$) vs. shNC. (h) The images of subcutaneous xenografts of OSLC (2×10^5) expressing red fluorescent protein (RFP) and shNC (left) and comparison of tumor weight of OSLCs expressing RFP and DNMT1 shRNA (right). The data were obtained from xenograft weighing results from 6 inoculation sites ($n = 6$). $^{*}p < 0.05$ vs. OSLCs expressing RFP. The images of immunohistochemistry of DNMT1 protein expression under an optical microscope (right) (scale bar, 50 μm).

mean ± standard deviation (SD). Comparisons with the control groups were performed using two-tailed Student's *t*-test. All the pairwise comparisons between the groups were analyzed by Tukey's post hoc test using one-way analysis of variance (abbreviated as one-way ANOVA). Significance was determined as $p < 0.05$.

3. Results

3.1. DNMT1 Activation and miR-34a Underexpression Are Associated with a Cancer Stem-like Cell (CSLC) Feature in the U2OS Cell Line. DNMT1 plays an essential role in CSLC feature maintenance and frequently decreased miR-34a expression in CSLCs [10–15, 22–25]. So, we initially compared the DNMT activation as well as miR-34a expression and promoter methylation between OSLCs (the sphere-forming U2OS cells) and U2OS cells (the monolayer U2OS cells). Among the DNMTs (DNMT1, DNMT3a, and DNMT3b), the activities of DNMT1 were markedly elevated by up to 23-fold in OSLCs when compared to U2OS cells (Figure 1(a)). Stronger DNMT1 activation was also shown in OSLCs than in U2OS cells (Figures 1(b) and 1(c)). In contrast, decreased expression and increased promoter methylation of miR-34a were observed in OSLCs relative to U2OS cells (Figures 1(d) and 1(e)). Altogether, these findings suggested that OSLCs exhibited an increased DNMT1 activity and decreased miR-34a expression relative to U2OS cells.

To estimate whether the OSLCs possess strong stemness, we next compared the capabilities of sphere formation and clonogenicity and expression levels of CSLC-related markers (CD133, CD44, and ABCG2) and pluripotent maintaining factors (Bmi1, Sox2, and Oct4) between OSLCs and U2OS cells. Enhanced capacities of sphere formation and clonogenicity (Figures 1(f) and 1(g)) and upregulated expressions of CD133, CD44, ABCG2, Bmi1, Sox2, and Oct4 (Figures 1(h) and 1(i)) were observed in OSLCs when

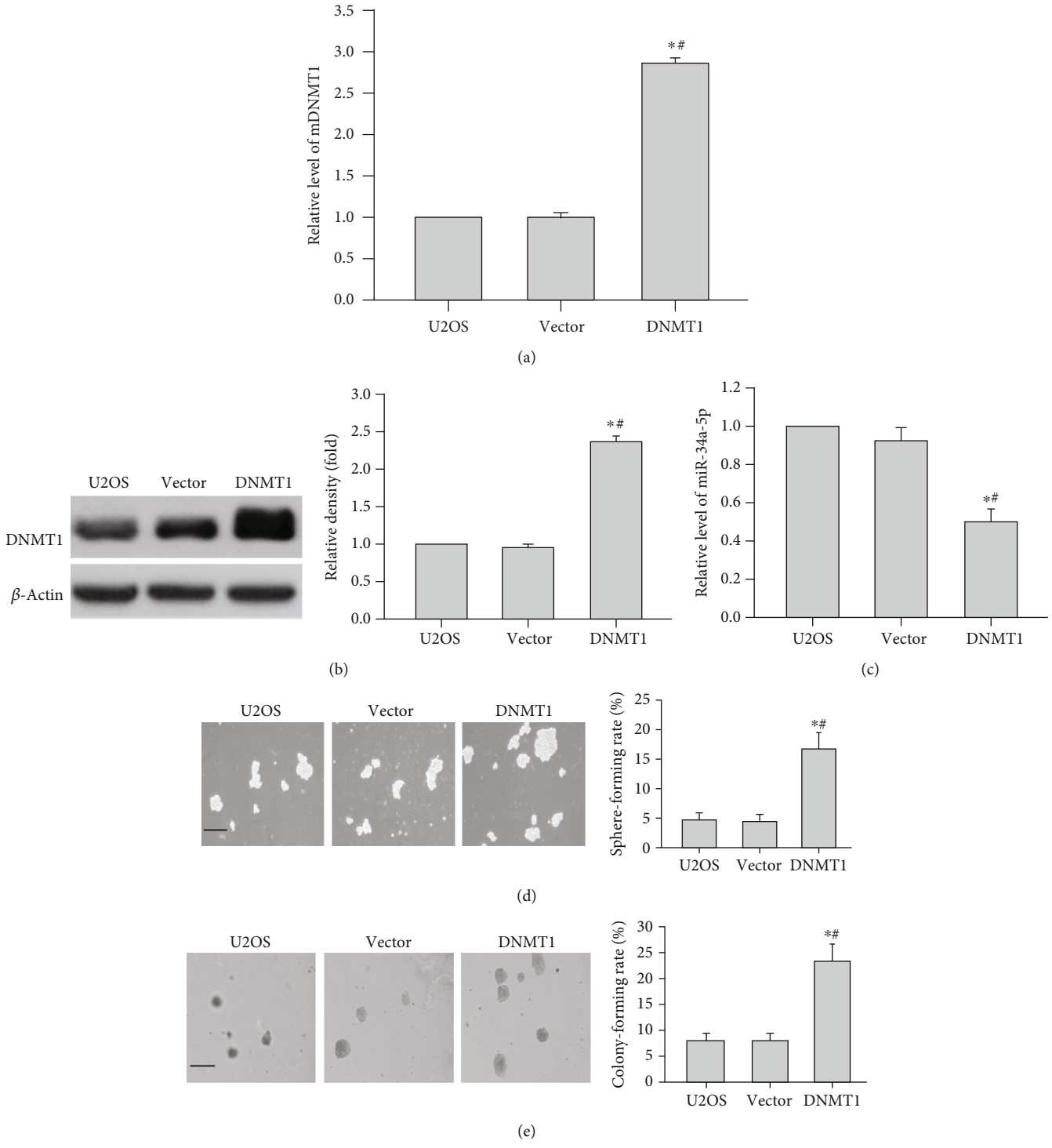

Figure 5: Continued.

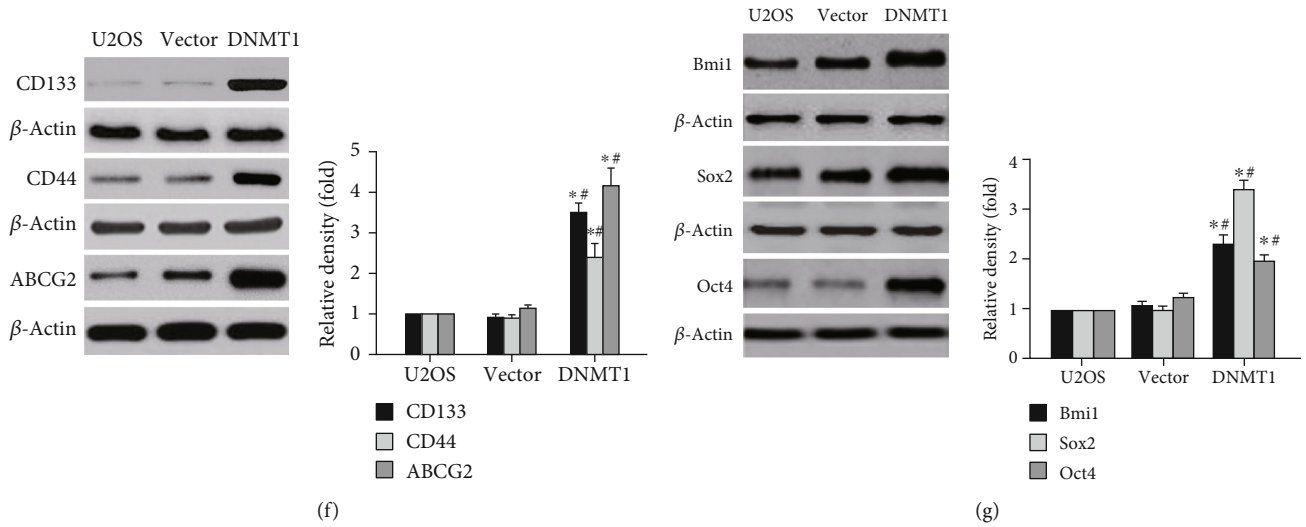

Figure 5: Effects of overexpressing DNMT1 on the stemness feature in U2OS cells. (a, b) DNMT1 mRNA and protein were detected by qRT-PCR and immunoblot in U2OS cells transfected with DNMT1 cDNA, with β-actin serving as a loading control. (c) qRT-PCR analyzed the miR-34a-5p level in U2OS cells transfected with DNMT1 cDNA. (d) Representative images of the spheres in U2OS cells transfected with DNMT1 cDNA (left) (scale bar, 200 μm) and the sphere-forming rates (right). (e) Representative images of the colonies in U2OS cells transfected with DNMT1 cDNA (left) (scale bar, 200 μm) and the colony-forming rates (right). (f) CD133, CD44, and ABCG2 proteins in U2OS cells transfected with DNMT1 cDNA (left) and their densitometric analysis (right), with β-actin serving as a loading control. (g) Bmi1, Sox2, and Oct4 were assessed in U2OS cells transfected with DNMT1 cDNA. $^{*}p < 0.05$ ($n = 3$) vs. U2OS cell; $^{\#}p < 0.05$ ($n = 3$) vs. vector control.

compared to U2OS cells. More importantly, the carcinogenicity *in vivo* was significantly heightened in OSLCs relative to U2OS cells (Figures 2(a)–2(d)). However, H&E staining revealed that the histological features of xenograft tumors induced by OSLCs were similar to those induced by the U2OS cells (Figure 2(e)). Collectively, these results indicated that the sphere-forming U2OS cells could enrich CSLCs and are used as OSLCs in further experiments.

3.2. DNMT Activation in the Acquisition and Maintenance of Stemness in OSLCs. To evaluate the effects of DNMT1 activation on miR-34a expression, miR-34a levels in OSLCs treated with or without the DNMT1 inhibitor 5-Aza-2′-deoxycytidine (Aza-dC) were evaluated. The reduced activity (Figure 3(a)) and expression of DNMT1 (Figures 3(b) and 3(c)) were consistent with the elevated miR-34a levels (Figure 3(d)) and reduced its promoter methylation (Figure 3(e)) in Aza-dC-treated OSLCs. Altogether, these data suggested that DNMT1 repression could increase miR-34a expression possibly by reducing its promoter methylation level in OSLCs.

To examine whether DNMT1 activation was required for the acquisition of a CSLC feature, we next examined the inhibition of DNMT1 activity by Aza-dC on the capacities of sphere formation and clonogenicity and the amounts of CD133, CD44, ABCG2, Bmi1, Sox2, and Oct4 in OSLCs. The results showed that Aza-dC declined the capacities of sphere formation and clonogenicity (Figures 3(f) and 3(g)) and the amounts of CD133, CD44, and ABCG2 (Figure 3(h)) as well as Bmi1, Sox2, and Oct4 (Figure 3(i)) of OSLCs, in a dose-dependent manner. Collectively, these results revealed that DNMT1 inhibition by Aza-dC effectively diminished the stemness of OSLCs.

To further determine the effects of DNMT1 activation on miR-34a expression, we generated OSLCs with shDNMT1 or shNC to examine DNMT1 and miR-34a expressions. Both mRNA and protein levels of DNMT1 in OSLCs expressing DNMT1 shRNA showed significant reduction (Figures 4(a) and 4(b)) and were consistent with the increased expression of miR-34a (Figure 4(c)) relative to NC shRNA or untreated control OSLCs. Altogether, our data showed that DNMT1 knockdown by transducing DNMT1 shRNA could upregulate miR-34a expression in OSLCs.

To further validate the effects of DNMT1 activation on the stemness, we assessed the knockdown of DNMT1 by expressing DNMT1 shRNA on the capacities of sphere formation and clonogenicity and the amounts of CD133, CD44, ABCG2, Bmi1, Sox2, and Oct4. The capacities of sphere formation and clonogenicity (Figures 4(d) and 4(e)) and the amounts of CD133, CD44, and ABCG2 (Figure 4(f)) as well as Bmi1, Sox2, and Oct4 (Figure 4(g)) were declined in OSLCs expressing DNMT1 shRNA relative to NC shRNA or untreated control OSLCs. More importantly, the *in vivo* carcinogenicity was significantly inhibited by DNMT1 knockdown in the nude mouse model of OSLCs (Figure 4(h)). Collectively, these results revealed that knockdown of DNMT1 by expressing DNMT1 shRNA effectively diminished the stemness of OSLCs.

To further confirm the influence of DNMT1 activation on miR-34a expression, U2OS cells with ectopic expression of DNMT1 were generated to compare the expressions of DNMT1 and miR-34a relative to vector control or untreated

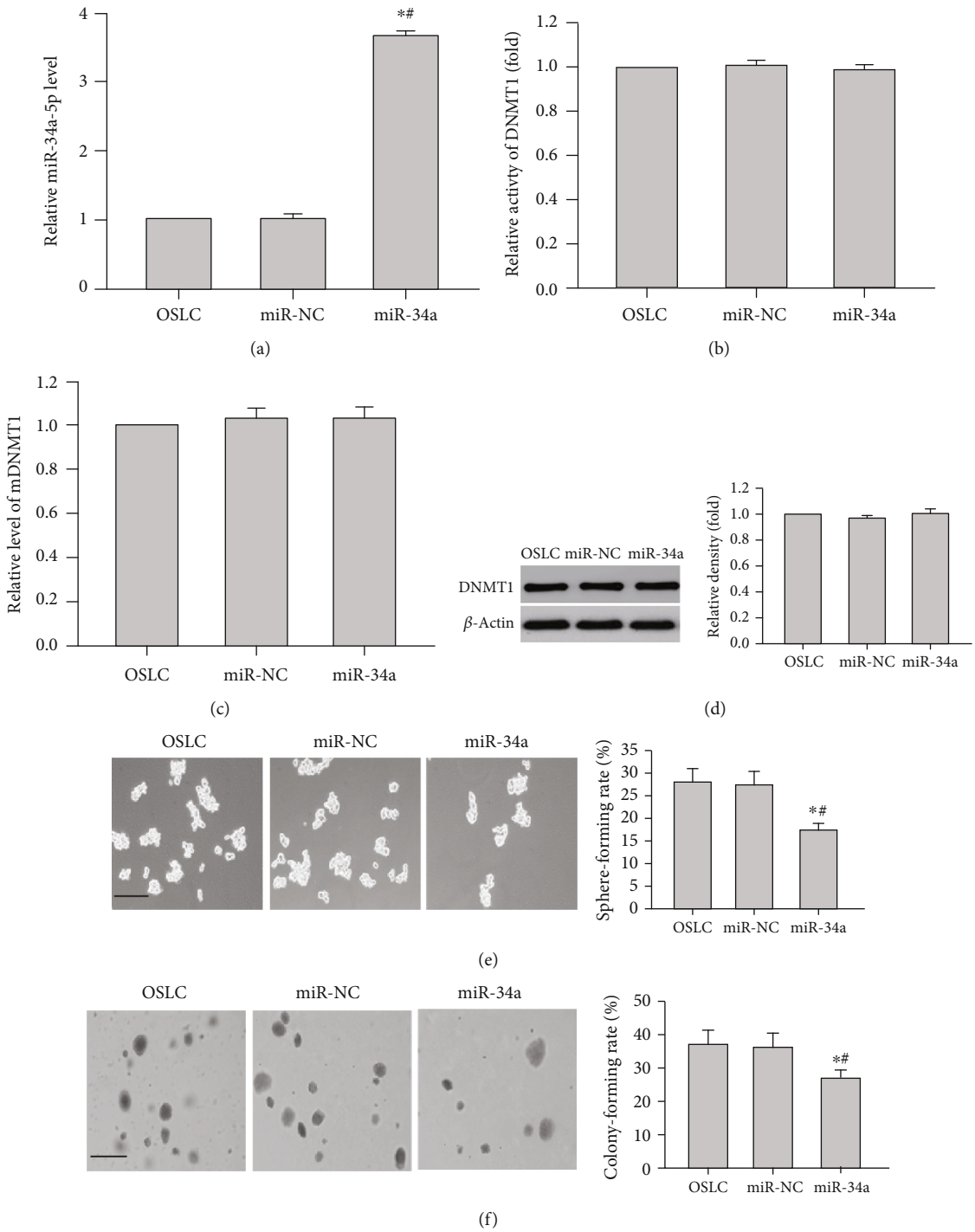

Figure 6: Continued.

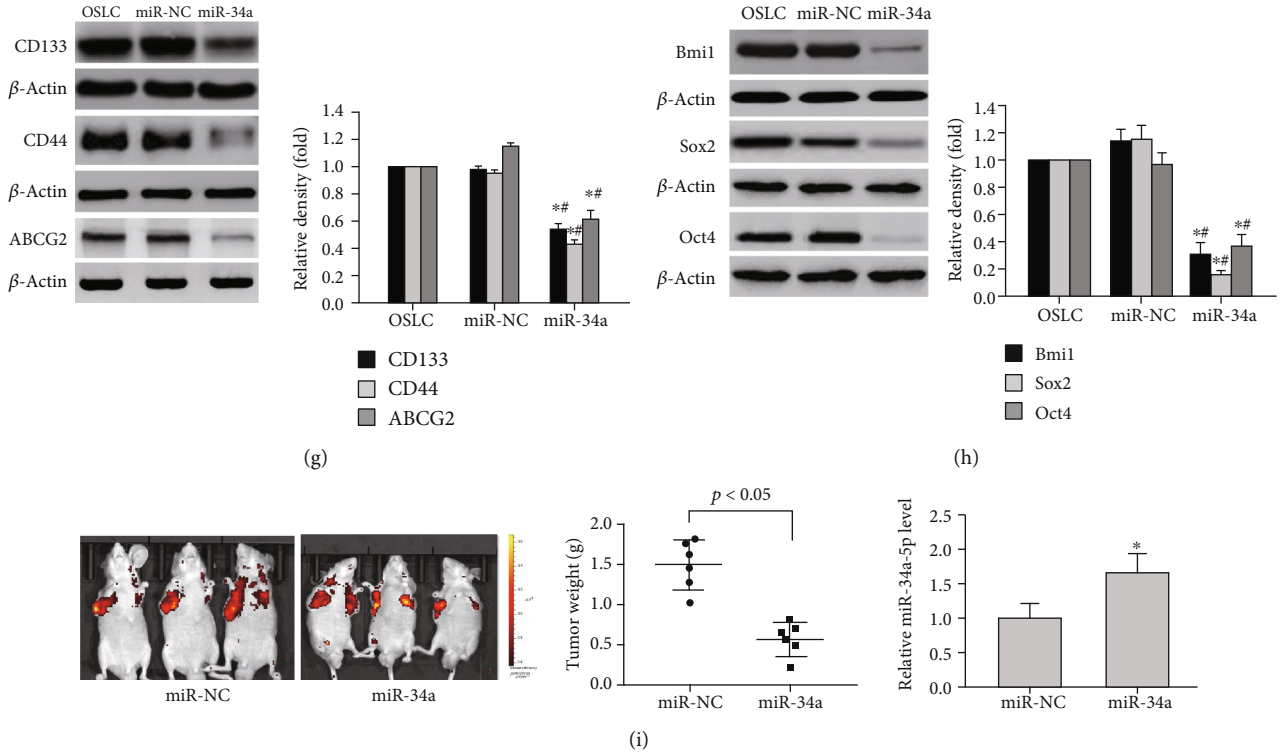

Figure 6: Effects of the miR-34a-5p mimic on the stemness feature in OSLCs. (a) qRT-PCR analyzed the level of miR-34a-5p in OSLCs transfected with miR-NC or miR-34a-5p mimic (miR-34a). (b, c) ELISA and qRT-PCR detected the activities and mRNA levels of DNMT1 in OSLCs transfected with miR-NC or miR-34a. (d) Immunoblot analyzed the expression of DNMT1 in OSLCs transfected with miR-NC or miR-34a, with β-actin serving as a loading control. (e) Representative images of the spheres in OSLCs transfected with miR-34a or with miR-NC and untreated cells serving as the controls (left) (scale bar, 200 μm) and the sphere-forming rate (right). (f) Representative images of the colonies in OSLCs transfected with miR-34a or with miR-NC and untreated cells serving as the controls (left) (scale bar, 200 μm) and the colony-forming rate (right). (g) CD133, CD44, and ABCG2 proteins in OSLCs transfected with miR-34a or miR-NC (left) and their densitometric analysis (right). (h) Bmi1, Sox2, and Oct4 in OSLCs transfected with miR-34a or miR-NC were assessed by qRT-PCR. $^{*}p < 0.05$ ($n = 3$) vs. OSLCs; $^{\#}p < 0.05$ ($n = 3$) vs. OSLCs transfected with miR-NC. (i) Images of subcutaneous xenografts of OSLCs (2×10^5) expressing red fluorescent protein (RFP) intratumorally injected with miR-NC or miR-34a (left) and comparison of tumor weight from OSLCs expressing RFP intratumorally injected with miR-NC or miR-34a (middle); and data were obtained from xenograft weighing results from 6 inoculation sites ($n = 6$). $^{*}p < 0.05$ vs. miR-NC. The expression level of miR-34a-5p of xenograft tumors intratumorally injected with NC or miR-34a (right). $^{*}p < 0.05$ vs. cells injected with miR-NC.

cells. Both mRNA and protein levels of DNMT1 were elevated (Figures 5(a) and 5(b)) and were consistent with decreased miR-34a (Figure 5(c)) in U2OS cells with ectopic expression of DNMT1 compared to vector control or untreated cells. Altogether, our data demonstrated that DNMT1 overexpression by transduction with DNMT1 cDNA downregulated miR-34a in U2OS cells.

Finally, we assessed whether DNMT1 overexpression enhances the capacities of sphere formation and clonogenicity and the amounts of CD133, CD44, ABCG2, Bmi1, Sox2, and Oct4 in U2OS cells. DNMT1 ectopic expression significantly contributed to the acquisition of stemness such as enhanced capacities of sphere formation and clonogenicity (Figures 5(d) and 5(e)) and increased amounts of CD133, CD44, ABCG2, Bmi1, Sox2, and Oct4 (Figures 5(f) and 5(g)) in U2OS cells with ectopic expression of DNMT1 relative to vector control or untreated cells. Collectively, these results demonstrated that DNMT1 constructive activation can promote the stemness in U2OS cells.

3.3. miR-34a Underexpression May Mediate the Promotion of Stemness Induced by DNMT1 Activation in OSLCs. To examine whether alteration of miR-34a expression affects DNMT1 activity and expression, OSLCs were transfected with a miR-34a mimic (miR-34a) or miR-34a mimic negative control (miR-NC). The results showed that miR-34a (Figure 6(a)) was upregulated, whereas the activity (Figure 6(b)) and expressions of DNMT1 (Figures 6(c) and 6(d)) showed no significant alterations in OSLCs transfected with miR-34a when compared to miR-NC or untreated control OSLCs. Altogether, our results indicated that miR-34a showed no effect on the DNMT1 activation of in OSLCs.

To assess the influences of miR-34a on the acquisition of stemness, we next examined whether miR-34a ectopic expression reduces the capacities of sphere formation and clonogenicity and the amounts of CD133, CD44, ABCG2, Bmi1, Sox2, and Oct4. The results revealed a decrease in the capacities of sphere formation and clonogenicity (Figures 6(e) and 6(f)) and the amounts of CD133, CD44,

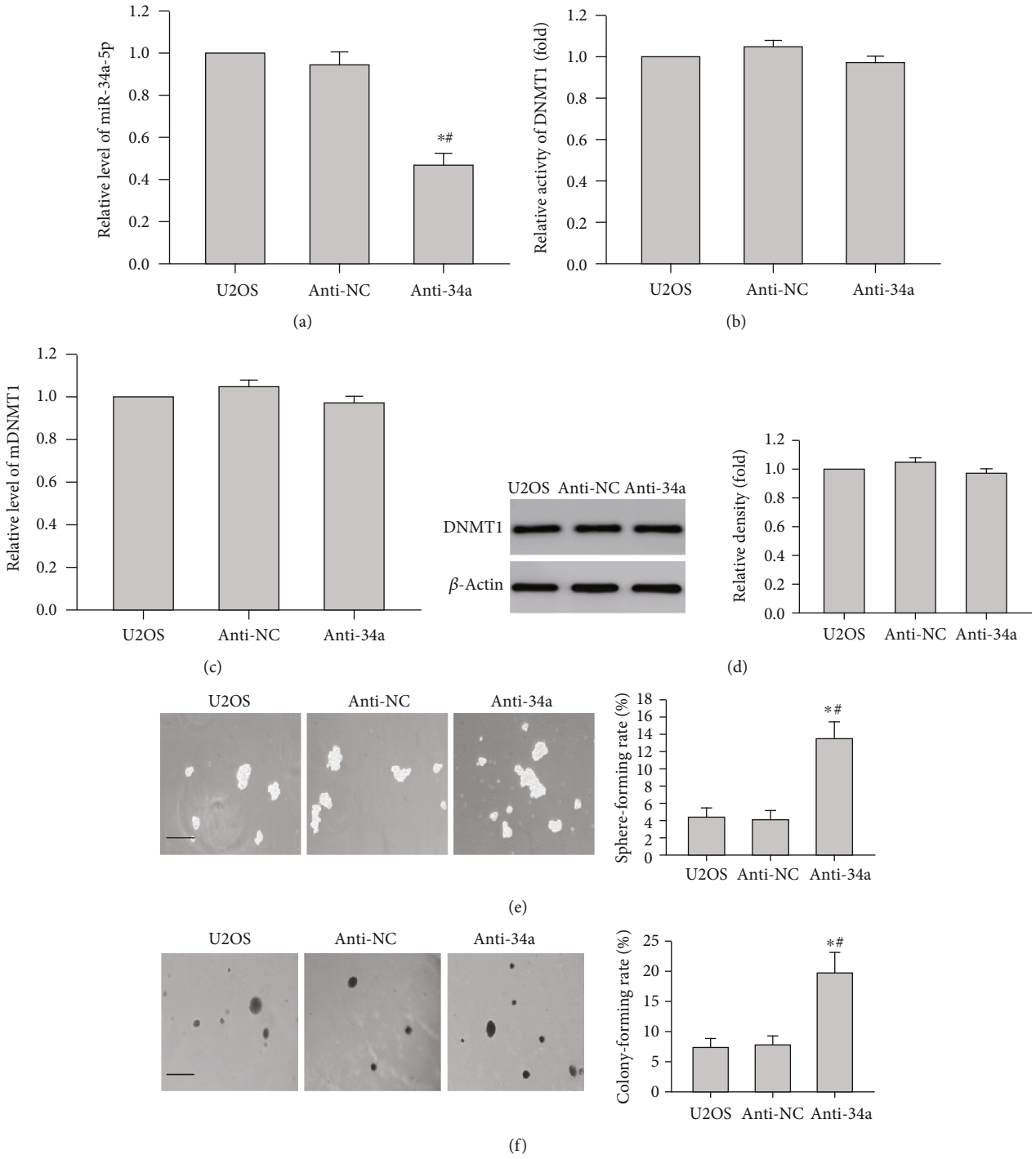

Figure 7: Continued.

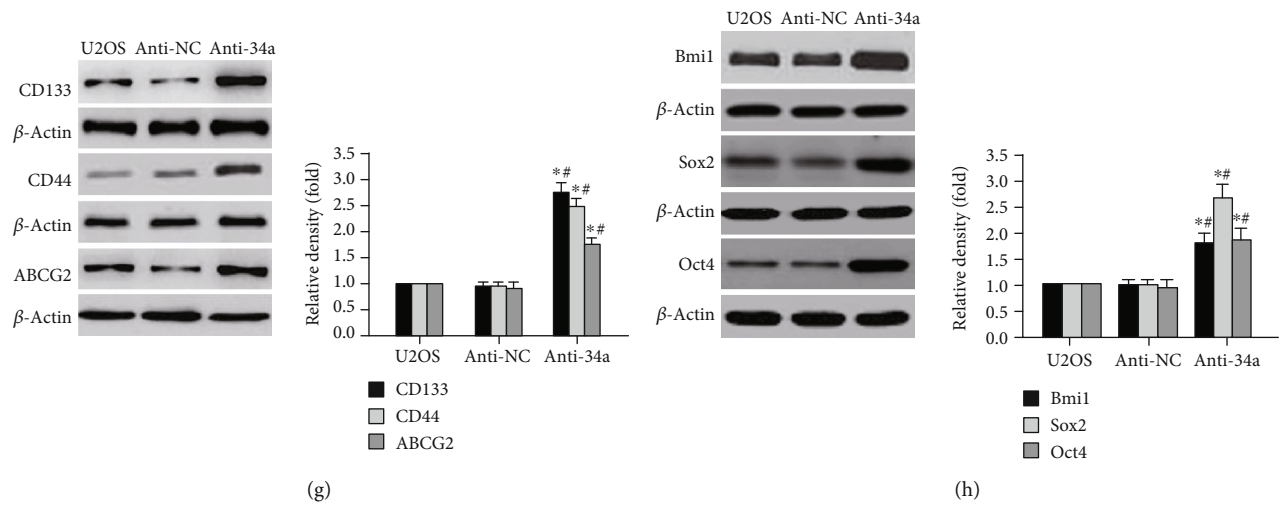

Figure 7: Effects of the miR-34a-5p inhibitor on the stemness feature in U2OS cells. (a) qRT-PCR analyzed the levels of miR-34a-5p in U2OS cells transfected with anti-NC or miR-34a inhibitor (anti-34a). $^{*}p < 0.05$ ($n = 3$) vs. U2OS cells; $^{\#}p < 0.05$ ($n = 3$) vs. anti-NC. (b, c) ELISA and qRT-PCR detected DNMT1 activities and mRNA in U2OS cells transfected with anti-NC or anti-34a. (d) Immunoblot analyzed the DNMT1 expression in U2OS cells transfected with anti-NC or anti-34a, with β-actin serving as a loading control. (e) Representative images of the spheres of U2OS cells transfected with anti-34a or with anti-NC and untreated U2OS cells serving as the controls (left) (scale bar, 200 μm) and the sphere-forming rates (right). (f) Representative images of the colony formation of U2OS cells transfected with anti-34a or with anti-NC and untreated U2OS cells serving as the controls (left) (scale bar, 200 μm) and the colony-forming rates (right). (g) CD133, CD44, and ABCG2 proteins in U2OS cells transfected with anti-34a or with anti-NC and untreated U2OS cells serving as the controls (left) and their densitometric analysis (right). (h) Bmi1, Sox2, and Oct4 of U2OS cells transfected with anti-34a or with anti-NC and untreated U2OS cells serving as the controls. $^{*}p < 0.05$ ($n = 3$) vs. U2OS cells; $^{\#}p < 0.05$ ($n = 3$) vs. U2OS cells transfected with anti-NC.

ABCG2, Bmi1, Sox2, and Oct4 (Figures 6(g) and 6(h)) in OSLCs transfected with miR-34a relative to miR-NC or untreated control. More importantly, the carcinogenicity *in vivo* was significantly inhibited in the OSLC nude mouse model by intratumoral injection with *agomir-34a* (Figure 6(i)). Collectively, these results indicated that stemness of OSLCs can be inhibited by miR-34a.

To further determine the influence of miR-34a on DNMT1 activation, U2OS cells were transfected with a miR-34a inhibitor (anti-34a) or miR-34a inhibitor negative control (Anti-NC). The results showed that miR-34a (Figure 7(a)) was significantly downregulated, whereas the activity (Figure 7(b)) and expressions of DNMT1 (Figures 7(c) and 7(d)) showed no differences in U2OS cells transfected with anti-34a relative to anti-NC or untreated U2OS cells. Altogether, our results indicated that miR-34a knockdown did not affect DNMT1 activation in U2OS cells.

To further evaluate the role of miR-34a in the acquisition of stemness, we examined whether anti-34a enhances the capacities of sphere formation and clonogenicity and the amounts of CD133, CD44, ABCG2, Bmi1, Sox2, and Oct4 in U2OS cells. The results showed an increase in the capacities of sphere formation and clonogenicity (Figures 7(e) and 7(f)) and the amounts of CD133, CD44, ABCG2, Bmi1, Sox2, and Oct4 (Figures 7(g) and 7(h)) in U2OS cells transfected with anti-34a relative to anti-NC or untreated cells. Collectively, our data indicated that the stemness of U2OS cells might depend on the miR-34a state in U2OS cells.

In order to provide convincing evidence that the inhibition of miR-34a by overexpressing DNMT1 promotes stemness, U2OS cells overexpressing DNMT1 were transfected with miR-34a followed by examining miR-34a and DNMT expression. Transfection of U2OS cells with miR-34a abrogated the overexpressing DNMT1-associated repression on miR-34a expression (Figure 8(a)), whereas elevated DNMT1 expression levels (Figures 8(b) and 8(c)) by DNMT1overexpression showed no changes. These results demonstrated that alterations of miR-34a expression were considered a downstream event of DNMT1 in U2OS cells.

To clearly prove that inhibition of miR34a by overexpressing DNMT1 promotes the stemness, U2OS cells overexpressing DNMT1 were transfected with miR-34a and the capacities of sphere formation and clonogenicity and the amounts of CD133, CD44, ABCG2, Bmi1, Sox2, and Oct4 were examined. The results demonstrated that transfection of U2OS cells with miR-34a reversed the overexpressing DNMT1-associated promotion on the stemness, such as enhancing the capacities of sphere formation and clonogenicity (Figures 8(d) and 8(e)) and the amounts of CD133, CD44, ABCG2, Bmi1, Sox2, and Oct4 (Figures 8(f) and 8(g)). Collectively, our data confirmed that miR-34a was one of the downstream effectors of DNMT1 for the acquisition and maintenance of stemness of U2OS cells.

4. Discussion

In the present study, the hypermethylation of the miR-34a promoter by abnormal activation of DNMT1 led to miR-34a underexpression in OSLCs compared to the corresponding OS cells, and miR-34a reexpression suppressed the stemness of OSLCs both *in vitro* and *in vivo*. Our results suggested that the DNMT1/miR-34a signaling axis exerts a crucial role in OS carcinogenesis, especially in the process of promoting and sustaining the stemness of OSLCs.

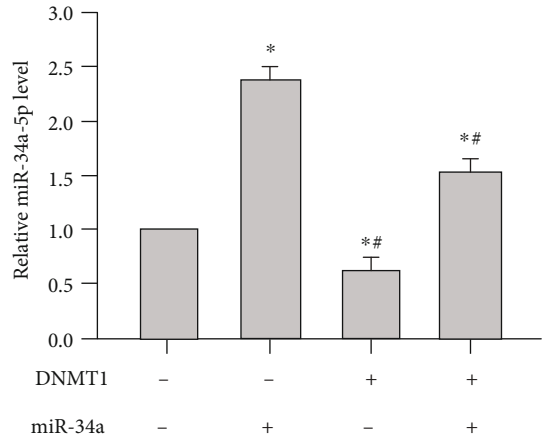

(a)

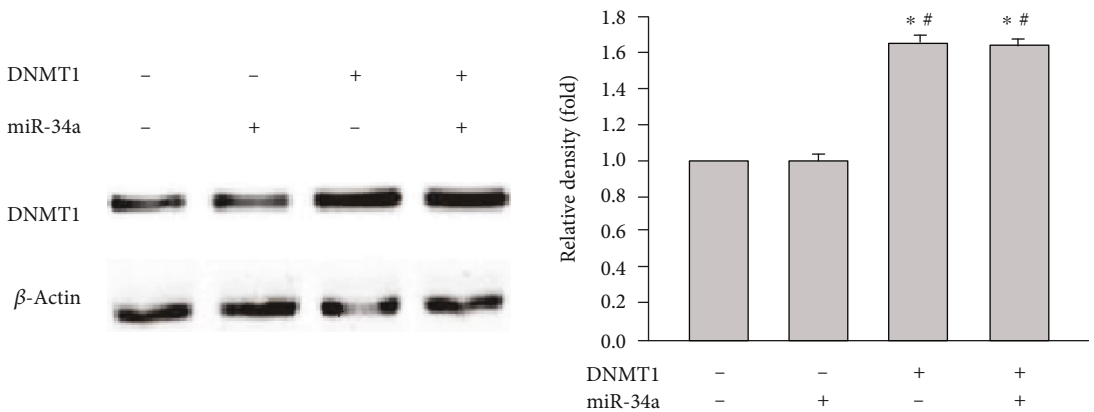

(b)

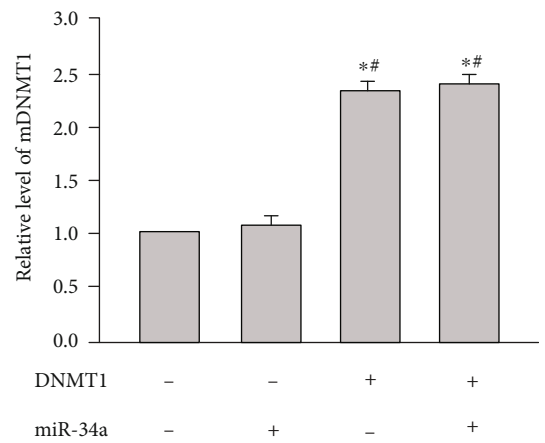

(c)

Figure 8: Continued.

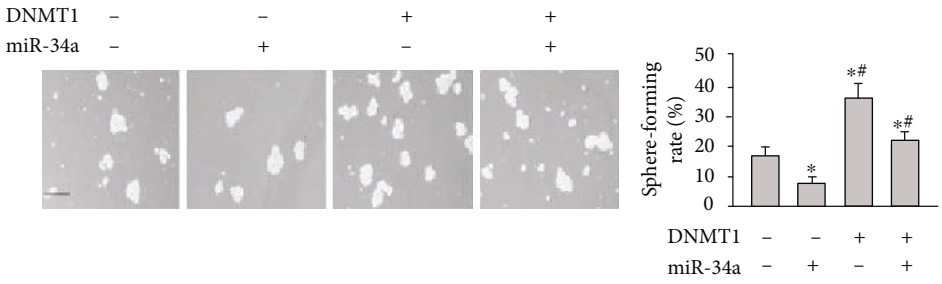

(d)

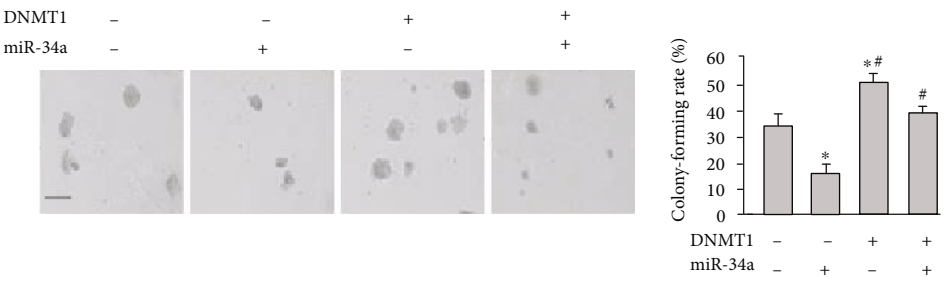

(e)

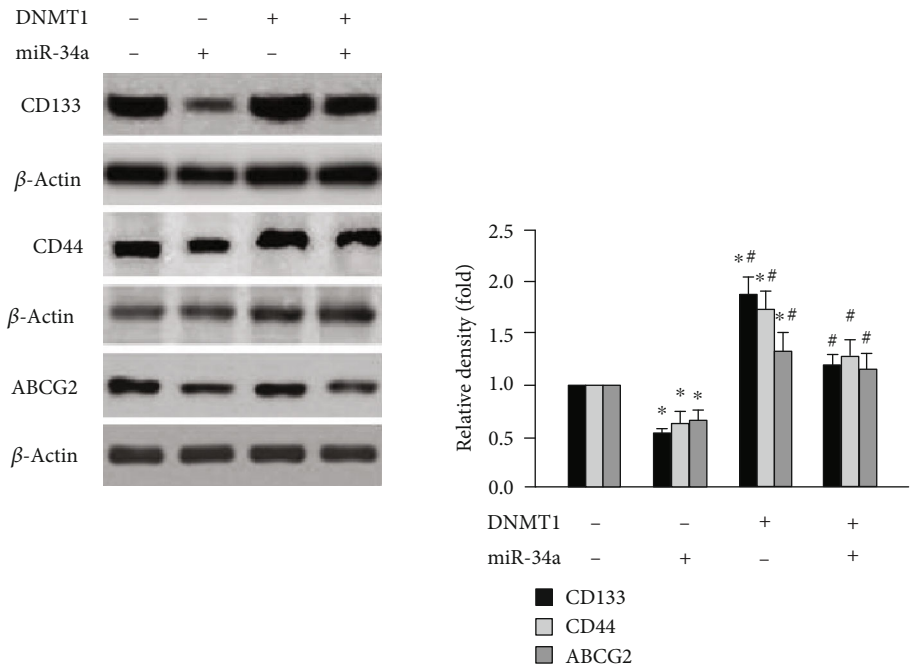

(f)

Figure 8: Continued.

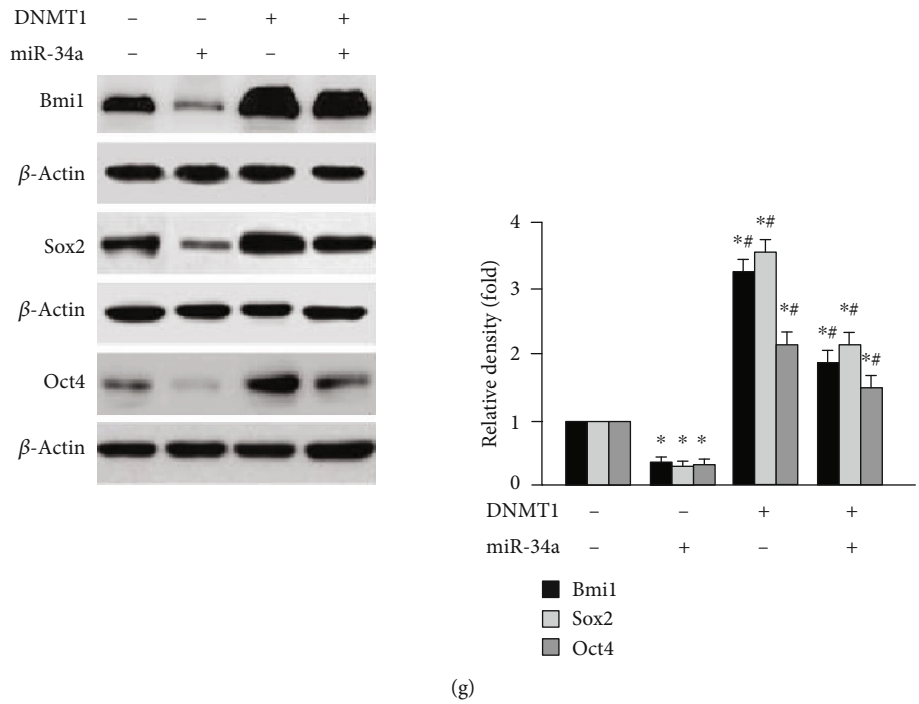

Figure 8: Effects of overexpressing DNMT1 combined with the miR-34a-5p mimic on stemness in U2OS cells. (a) qRT-PCR analyzed the effect of the miR-34a mimic on the miR-34a expression in U2OS cells overexpressing DNMT1. (b, c) Immunoblotting and qRT-PCR detected the DNMT1 protein and mRNA in U2OS cells overexpressing DNMT1 (DNMT1) transfected with the miR-34a mimic (miR-34a) and their densitometric analysis (right), with β-actin serving as a loading control. $^{*}p < 0.05$ ($n = 3$) vs. U2OS cells; $^{\#}p < 0.05$ ($n = 3$) vs. U2OS cells transfected with miR-34a. (d) Representative images of the spheres of U2OS cells overexpressing DNMT1 transfected with miR-34a (left) (scale bar, 200 μm) and the sphere-forming rates (right). (e) Representative images of the colonies of U2OS cells overexpressing DNMT1 transfected with miR-34a (left) (scale bar, 200 μm) and the colony-forming rates (right). (f) CD133, CD44, and ABCG2 proteins of U2OS cells overexpressing DNMT1 transfected with miR-34a (left) and their densitometric analysis (right). (g) Bmi1, Sox2, and Oct4 of U2OS cells overexpressing DNMT1 transfected with miR-34a. $^{*}p < 0.05$ ($n = 3$) vs. U2OS cells; $^{\#}p < 0.05$ ($n = 3$) vs. U2OS cells transfected with miR-34a.

Aberrant expressions of miRNAs are involved in the regulation of stemness in various cancers by controlling stemness-related gene expressions [10, 11, 14, 34–40]. miR-34a has been recognized as a tumor-suppressive miRNA and reduced carcinogenesis in a variety of cancers, including OS [30–33]. Underexpression of miR-34a has been implicated in maintaining the stemness of CSLCs [14, 15], especially in OS cells [10, 11]. In the current study, we demonstrated that miR-34a was underexpressed in OSLCs compared with corresponding U2OS cells, and miR-34a reexpression could repress the capacities of sphere and clonogenic formation as well as downregulated stemness-related genes including CD133, CD44, ABCG2, Bmi1, Sox2, and Oct4. These results underlined that miR-34a mimics or modulator upregulated miR-34a, which might be a promising agent against human OS that targets OSLCs.

The pivotal role of DNMT1 in the regulation and stemness of CSLCs has been well documented in various tumors, including leukemia [41], breast cancer [42], hepatocelluar cancer [43], non-small-cell lung cancer [44], and pancreatic adenocarcinoma [45] and OS [46]. Interestingly, the study by Peng et al. [33] showed that DNMT1 overexpression resulted in dramatic downregulation by hypermethylation of the miR-34a promoter, which promoted the stemness in breast cancer. According to a study, miR-148a inhibited the differentiation and proliferation of CSLCs derived from primary OS cells by directly targeting DNMT1 [29]. However, few other studies have examined the promotion of stemness by downregulated miR-34a through aberrant expression of DNMT1 in OSLCs and OS cells. The present study provided evidence that DNMT1 was significantly activated, leading to the underexpression of miR-34a through hypermethylation of its promoter in OSLCs when compared with corresponding OS cells. Meanwhile, a higher carcinogenicity was observed as indicated by stronger capacities of sphere and clonogenic formation, and stronger stemness was also displayed as demonstrated by highly expressed stemness-related genes such as CD133, CD44, ABCG2, Bmi1, Sox2, and Oct4 *in vitro* in OSLCs than in the corresponding OS cells. Our results suggested for the first time that the DNMT1/miR-34a axis substantially promoted the stemness in OSLCs and highlighted the role of the DNMT1/miR-34a axis in the treatment for OS targeting OSLCs.

In OS cells, many studies showed that miR-34a targeted a variety of oncogenes including certain stemness-related genes such as CD44 [14] and Sox2 [10]. Zhao et al. [47] utilized genetically engineered pre-miRNA-34a prodrug to demonstrate repression of miR-34a on tumor growth of an orthotopic OS xenograft nude model *in vivo*. Although that the targets of miR-34a repressed the stemness of OSLCs

requires further exploration, we here demonstrated that the tumor growth in subcutaneous nude mouse xenograft models of OSLCs was suppressed by treatment with either the DNMT1 inhibitor Aza-dC or *agomir-34a*. Our results suggested that phenocopied miR-34a or inactivated DNMT1 or both may be a promising potential approach targeting OSLCs for human OS treatment.

In summary, our study has gained insights into DNMT1 overexpression that led to miR-34a methylation silence, promoting the stemness of OS cells and their derived OSLCs. It is appealing to consider that the epigenetic-based reprogramming applications in the treatment of solid tumors can promote the development of alternative therapies targeting OSLCs for inoperable or drug-resistant OS.

Data Availability

No data were used to support this study.

Conflicts of Interest

The authors declare that they have no conflict of interest.

Acknowledgments

This study was supported by the National Natural Science Foundation of China (Nos. 81301894 and 81302249).

Supplementary Materials

(1) The supplementary table about mRNA primer sequence of DNMT1 and β-actin. (2) The supplementary table about primer sequence of miR-34a-5p and U6. (3) The supplementary table about primer sequence of miR-34a-5p-M and miR-34a-5p-U. *(Supplementary Materials)*

References

[1] R. L. Siegel, K. D. Miller, and A. Jemal, "Cancer statistics, 2016," *CA: A Cancer Journal for Clinicians*, vol. 66, no. 1, pp. 7–30, 2016.

[2] S. Ferrari and M. Serra, "An update on chemotherapy for osteosarcoma," *Expert Opinion on Pharmacotherapy*, vol. 16, pp. 2727–2736, 2015.

[3] W. Liu, Z. Zhao, Y. Wang et al., "Dioscin inhibits stem-cell-like properties and tumor growth of osteosarcoma through Akt/GSK3/β-catenin signaling pathway," *Cell Death & Disease*, vol. 9, p. 343, 2018.

[4] A. Abarrategi, J. Tornin, L. Martinez-Cruzado et al., "Osteosarcoma: cells-of-origin, cancer stem cells, and targeted therapies," *Stem Cells International*, vol. 2016, Article ID 3631764, 2016.

[5] D. Albino, G. Civenni, C. Dallavalle et al., "Activation of the Lin28/let-7 axis by loss of ESE3/EHF promotes a tumorigenic and stem-like phenotype in prostate cancer," *Cancer Research*, vol. 76, pp. 3629–3643, 2016.

[6] C. De Vito, N. Riggi, S. Cornaz et al., "A TARBP2-dependent miRNA expression profile underlies cancer stem cell properties and provides candidate therapeutic reagents in Ewing sarcoma," *Cancer Cell*, vol. 21, pp. 807–821, 2012.

[7] H. Hermeking, "MicroRNAs in the p53 network: micromanagement of tumour suppression," *Nature Reviews Cancer*, vol. 12, pp. 613–626, 2012.

[8] A. Parafioriti, C. Bason, E. Armiraglio et al., "Ewing's sarcoma: an analysis of miRNA expression profiles and target genes in paraffin-embedded primary tumor tissue," *International Journal of Molecular Sciences*, vol. 17, 2016.

[9] Y. Li, P. Gong, J. X. Hou et al., "miR-34a regulates multidrug resistance via positively modulating OAZ2 signaling in colon cancer cells," *Journal of Immunology Research*, vol. 2018, Article ID 7498514, 13 pages, 2018.

[10] Y. Zhang, Y. Pan, C. Xie, and Y. Zhang, "miR-34a exerts as a key regulator in the dedifferentiation of osteosarcoma via PAI-1–Sox2 axis," *Cell Death & Disease*, vol. 9, 2018.

[11] Y. Zou, Y. Huang, J. Yang, J. Wu, and C. Luo, "miR-34a is downregulated in human osteosarcoma stem-like cells and promotes invasion, tumorigenic ability and self-renewal capacity," *Molecular Medicine Reports*, vol. 15, pp. 1631–1637, 2017.

[12] L. Wang, P. Bu, Y. Ai et al., "A long non-coding RNA targets microRNA miR-34a to regulate colon cancer stem cell asymmetric division," *eLife*, vol. 5, 2016.

[13] P. Bonetti, M. Climent, F. Panebianco et al., "Dual role for miR-34a in the control of early progenitor proliferation and commitment in the mammary gland and in breast cancer," *Oncogene*, vol. 38, no. 3, pp. 360–374, 2018.

[14] C. Liu, K. Kelnar, B. Liu et al., "The microRNA miR-34a inhibits prostate cancer stem cells and metastasis by directly repressing CD44," *Nature Medicine*, vol. 17, pp. 211–215, 2011.

[15] Q. Zhang, J. Zhuang, Y. Deng et al., "miR34a/GOLPH3 axis abrogates urothelial bladder cancer chemoresistance via reduced cancer stemness," *Theranostics*, vol. 7, pp. 4777–4790, 2017.

[16] S. Xu, Y. Yue, S. Zhang et al., "STON2 negatively modulates stem-like properties in ovarian cancer cells via DNMT1/MUC1 pathway," *Journal of Experimental & Clinical Cancer Research*, vol. 37, no. 1, 2018.

[17] A. A. Samadani, S. E. Norollahi, A. Rashidy-Pour et al., "Cancer signaling pathways with a therapeutic approach: an overview in epigenetic regulations of cancer stem cells," *Biomedicine & Pharmacotherapy*, vol. 108, pp. 590–599, 2018.

[18] Q. Li, C. Dong, J. Cui, Y. Wang, and X. Hong, "Over-expressed lncRNA HOTAIRM1 promotes tumor growth and invasion through up-regulating HOXA1 and sequestering G9a/EZH2/Dnmts away from the HOXA1 gene in glioblastoma multiforme," *Journal of Experimental & Clinical Cancer Research*, vol. 37, 2018.

[19] Y. Wang, H. Cardenas, F. Fang et al., "Epigenetic targeting of ovarian cancer stem cells," *Cancer Research*, vol. 74, pp. 4922–4936, 2014.

[20] R. Pathania, S. Ramachandran, S. Elangovan et al., "DNMT1 is essential for mammary and cancer stem cell maintenance and tumorigenesis," *Nature Communications*, vol. 6, 2015.

[21] N. Zhang, Y. Liu, Y. Wang, M. Zhao, L. Tu, and F. Luo, "Decitabine reverses TGF-β1-induced epithelial–mesenchymal transition in non-small-cell lung cancer by regulating miR-200/ZEB axis," *Drug Design, Development and Therapy*, vol. 11, pp. 969–983, 2017.

[22] Z. Peng, W. Zhou, C. Zhang, H. Liu, and Y. Zhang, "Curcumol controls choriocarcinoma stem-like cells self-renewal via

repression of DNA methyltransferase (DNMT)- and histone deacetylase (HDAC)-mediated epigenetic regulation," *Medical Science Monitor*, vol. 24, pp. 461–472, 2018.

[23] A. P. Lombard, B. A. Mooso, S. J. Libertini et al., "miR-148a dependent apoptosis of bladder cancer cells is mediated in part by the epigenetic modifier DNMT1," *Molecular Carcinogenesis*, vol. 55, pp. 757–767, 2016.

[24] Y. Deng, F. Zhao, L. Hui et al., "Suppressing miR-199a-3p by promoter methylation contributes to tumor aggressiveness and cisplatin resistance of ovarian cancer through promoting DDR1 expression," *Journal of Ovarian Research*, vol. 10, 2017.

[25] F. Yang, K. He, L. Huang, L. Zhang, A. Liu, and J. Zhang, "Casticin inhibits the activity of transcription factor Sp1 and the methylation of RECK in MGC803 gastric cancer cells," *Experimental and Therapeutic Medicine*, vol. 13, pp. 745–750, 2017.

[26] F. Chen, N. Luo, Y. Hu, X. Li, and K. Zhang, "MiR-137 suppresses triple-negative breast cancer stemness and tumorigenesis by perturbing BCL11A-DNMT1 interaction," *Cellular Physiology and Biochemistry*, vol. 47, pp. 2147–2158, 2018.

[27] S. Jili, L. Eryong, L. Lijuan, and Z. Chao, "RUNX3 inhibits laryngeal squamous cell carcinoma malignancy under the regulation of miR-148a-3p/DNMT1 axis," *Cell Biochemistry and Function*, vol. 34, pp. 597–605, 2016.

[28] S. Zagorac, S. Alcala, B. G. Fernandez et al., "DNMT1 inhibition reprograms pancreatic cancer stem cells via upregulation of the miR-17-92 cluster," *Cancer Research*, vol. 76, no. 15, pp. 4546–4558, 2016.

[29] C. Yuewen, Z. Yongfang, G. Wei et al., "Bufalin inhibits the differentiation and proliferation of cancer stem cells derived from primary osteosarcoma cells through mir-148a," *Cellular Physiology & Biochemistry*, vol. 36, pp. 1186–1196, 2015.

[30] U. Schirmer, K. Doberstein, A.-K. Rupp et al., "Role of miR-34a as a suppressor of L1CAM in endometrial carcinoma," *Oncotarget*, vol. 5, pp. 462–472, 2014.

[31] X. Peng, H. Chang, Y. Gu et al., "3,6-Dihydroxyflavone suppresses breast carcinogenesis by epigenetically regulating miR-34a and miR-21," *Cancer Prevention Research*, vol. 8, pp. 509–517, 2015.

[32] F. Chamani, M. Sadeghizadeh, M. Masoumi, and S. Babashah, "Evaluation of MiR-34 family and DNA methyltransferases 1, 3A, 3B gene expression levels in hepatocellular carcinoma following treatment with Dendrosomal nanocurcumin," *Asian Pacific Journal of Cancer Prevention*, vol. 17, pp. 219–224, 2016.

[33] X. Peng, H. Chang, J. Chen, Q. Zhang, X. Yu, and M. Mi, "3,6-Dihydroxyflavone regulates microRNA-34a through DNA methylation," *BMC Cancer*, vol. 17, 2017.

[34] A. Y. So, J. W. Jung, S. Lee, H. S. Kim, and K. S. Kang, "DNA methyltransferase controls stem cell aging by regulating BMI1 and EZH2 through microRNAs," *PLoS One*, vol. 6, 2011.

[35] N. Bucay, K. Sekhon, T. Yang et al., "MicroRNA-383 located in frequently deleted chromosomal locus 8p22 regulates CD44 in prostate cancer," *Oncogene*, vol. 36, pp. 2667–2679, 2017.

[36] L. Zhou, L. C. Zhao, N. Jiang et al., "MicroRNA miR-590-5p inhibits breast cancer cell stemness and metastasis by targeting SOX2," *European Review for Medical and Pharmacological Sciences*, vol. 21, pp. 87–94, 2017.

[37] A. R. Göhring, S. Reuter, J. H. Clement et al., "Human microRNA-299-3p decreases invasive behavior of cancer cells by downregulation of Oct4 expression and causes apoptosis," *PLoS One*, vol. 12, 2017.

[38] J. F. Zeng, X. Q. Ma, L. P. Wang, and W. Wang, "MicroRNA-145 exerts tumor-suppressive and chemo-resistance lowering effects by targeting CD44 in gastric cancer," *World Journal of Gastroenterology*, vol. 23, pp. 2337–2345, 2017.

[39] Y. C. Lu, A. J. Cheng, L. Y. Lee et al., "MiR-520b as a novel molecular target for suppressing stemness phenotype of head-neck cancer by inhibiting CD44," *Scientific Reports*, vol. 7, no. 1, 2017.

[40] N. Patel, K. R. Garikapati, V. K. K. Makani et al., "Regulating BMI1 expression via miRNAs promote mesenchymal to epithelial transition (MET) and sensitizes breast cancer cell to chemotherapeutic drug," *PLoS One*, vol. 13, 2018.

[41] T. Rahmani, M. Azad, B. Chahardouli, H. Nasiri, M. Vatanmakanian, and S. Kaviani, "Patterns of DNMT1 promoter methylation in patients with acute lymphoblastic leukemia," *International Journal of Hematology-Oncology and Stem Cell Research*, vol. 11, pp. 172–177, 2017.

[42] N. Chen, G. Zhao, X. Yan et al., "A novel FLI1 exonic circular RNA promotes metastasis in breast cancer by coordinately regulating TET1 and DNMT1," *Genome Biology*, vol. 19, 2018.

[43] X. Gao, Y. Sheng, J. Yang et al., "Osteopontin alters DNA methylation through up-regulating DNMT1 and sensitizes CD133+/CD44+ cancer stem cells to 5 azacytidine in hepatocellular carcinoma," *Journal of Experimental & Clinical Cancer Research*, vol. 37, 2018.

[44] C. C. Liu, J. H. Lin, T. W. Hsu et al., "IL-6 enriched lung cancer stem-like cell population by inhibition of cell cycle regulators via DNMT1 upregulation," *International Journal of Cancer*, vol. 136, pp. 547–559, 2015.

[45] Q. Xiao, D. Zhou, A. A. Rucki et al., "Cancer-associated fibroblasts in pancreatic cancer are reprogrammed by tumor-induced alterations in genomic DNA methylation," *Cancer Research*, vol. 76, pp. 5395–5404, 2016.

[46] H. Zhao, B. Ma, Y. Wang et al., "miR-34a inhibits the metastasis of osteosarcoma cells by repressing the expression of CD44," *Oncology Reports*, vol. 29, pp. 1027–1036, 2013.

[47] Y. Zhao, M. J. Tu, W. P. Wang, J. X. Qiu, A. X. Yu, and A. M. Yu, "Genetically engineered pre-microRNA-34a prodrug suppresses orthotopic osteosarcoma xenograft tumor growth via the induction of apoptosis and cell cycle arrest," *Scientific Reports*, vol. 6, 2016.